NACA RM L50F08

NACA

RESEARCH MEMORANDUM

EFFECTS OF VARYING THE SIZE AND LOCATION OF TRAILING-EDGE FLAP-TYPE CONTROLS ON THE AERODYNAMIC CHARACTERISTICS OF AN UNSWEPT WING AT A MACH NUMBER OF 1.9

By Meade H. Mitchell, Jr.

Langley Aeronautical Laboratory
Langley Air Force Base, Va.

NATIONAL ADVISORY COMMITTEE
FOR AERONAUTICS
WASHINGTON

August 16, 1950

NATIONAL ADVISORY COMMITTEE FOR AERONAUTICS

RESEARCH MEMORANDUM

EFFECTS OF VARYING THE SIZE AND LOCATION OF TRAILING-EDGE FLAP-TYPE CONTROLS ON THE AERODYNAMIC CHARACTERISTICS OF AN UNSWEPT WING AT A MACH NUMBER OF 1.9

By Meade H. Mitchell, Jr.

SUMMARY

An investigation has been made in the Langley 9- by 12-inch supersonic blowdown tunnel at a Mach number of 1.9 and a Reynolds number of 2.3×10^6 to determine the effects of flap size and location on an unswept semispan wing in combination with a half-fuselage. The wing had an aspect ratio of 2.5, a taper ratio of 0.625, and 6-percent-thick modified double-wedge airfoil sections. Flap configurations included 25-, 35-, and 45-percent-chord plain flaps of various spans located at various spanwise stations.

The values of rolling-moment coefficient and the increments in lift coefficient caused by flap deflection varied linearly with flap deflection for each flap configuration and were about additive for adjacent flap-span segments. The rate of change in the rolling-effectiveness parameter C_{l_δ} with flap span, brought about by progressive removal of the outboard end of the flap, decreased slightly as the span decreased. A slight increase was noted in the rate of change of C_{l_δ} with flap chord as the chord increased.

For most configurations, theory predicted the trends in flap characteristics as influenced by changes in chord, span, and spanwise location of the flaps; however, theoretical effectiveness values were higher than the experimental results by 10 to 30 percent for rolling moment and 0 to 30 percent for lift and pitching moment. For flaps located adjacent to the fuselage, the calculated effectiveness sometimes fell below experiment, probably because theory did not consider the increased rate of flow near the fuselage.

INTRODUCTION

General trends of control characteristics at supersonic speeds cannot always be predicted by simple theory. As an example of the unexpected, the test results at supersonic speeds of reference 1 have shown that, for at least one set of design conditions, the location of a constant-span trailing-edge aileron should be moved inboard as the wing is swept back in order to achieve maximum rolling effectiveness. Such information points out the need for detailed experimental information concerning the optimum size and location of supersonic control surfaces, especially as affected by wing geometry and Mach number. An experimental investigation has therefore been started in the Langley 9- by 12-inch supersonic blow-down tunnel to study the effects of some of the design parameters on control effectiveness.

As part of this investigation, several flap-type control arrangements have been tested on an unswept semispan wing in the presence of a fuselage. The wing had an aspect ratio of 2.5, a taper ratio of 0.625, and 6-percent-thick modified double-wedge airfoil sections. The chords and spans of the flaps varied from 25 to 45 percent of the wing chord and from 25 to 75 percent of the wing semispan, respectively, and were tested at various spanwise locations. The investigation was carried out at a Mach number of 1.9 and a Reynolds number of 2.3×10^6 through angles of attack varying from -2° to 4°. Flaps were deflected from 0° to 15°.

Five-component force data are presented, and the experimental values of flap lift, rolling-moment, and pitching-moment effectiveness are compared with theory.

COEFFICIENTS AND SYMBOLS

All data are presented with respect to the wind axes.

C_L lift coefficient $\left(\frac{\text{Lift}}{qS}\right)$

C_D drag coefficient $\left(\frac{\text{Drag}}{qS}\right)$

C_m pitching-moment coefficient $\left(\frac{\text{Pitching moment about } 0.5\bar{c}}{qS\bar{c}}\right)$

$C_{l_{gross}}$ gross rolling-moment coefficient $\left(\frac{\text{Rolling moment of the semispan wing}}{2qSb}\right)$

$C_{n_{gross}}$ gross yawing-moment coefficient $\left(\frac{\text{Yawing moment of the semispan wing}}{2qSb}\right)$

C_l rolling-moment coefficient $\left(C_{l_{gross}} - C_{l_{gross(\delta=0^\circ)}}\right)$

ΔC_l, ΔC_m increment in coefficient due to control-surface deflection

Δp increment in pressure

q free-stream dynamic pressure

S exposed semispan wing area (10.00 sq in.)

$\bar{c}$ mean aerodynamic chord of exposed wing area (3.13 in.)

c local wing chord

c_f local control-surface chord

b twice distance from wing root to wing tip (8.13 in.)

b_f control-surface span

y_f spanwise location of inboard end of control surface

α angle of attack relative to free-stream direction

δ control-surface deflection measured in a plane normal to hinge line (positive with trailing edge deflected down)

R Reynolds number based on $\bar{c}$

C_{L_α} rate of change in lift coefficient with angle of attack $\left(\frac{\partial C_L}{\partial \alpha}\right)$

C_{L_δ} rate of change in lift coefficient with control-surface deflection $\left(\frac{\partial C_L}{\partial \delta}\right)$

C_{m_δ} rate of change in pitching-moment coefficient with control-surface deflection $\left(\frac{\partial C_m}{\partial \delta}\right)$

C_{l_δ} rate of change in rolling-moment coefficient with control-surface deflection $\left(\frac{\partial C_l}{\partial \delta}\right)$

MODEL AND TESTS

Model

A photograph of the semispan wing and the half-fuselage installed in the test section is shown in figure 1. The geometry of the configuration is presented in figure 2 (the fuselage ordinates are the same as those presented in fig. 3). The wing was unswept at the midchord line and had a taper ratio of 0.625 and an aspect ratio of 2.5, based on the wing area (13.12 sq in.) which included that portion of the wing enclosed by the fuselage. The 30-percent-chord wedge-shaped leading and trailing edges had included wedge angles of 11.43° measured streamwise. The center 40 percent of the wing chord had a constant 6-percent-chord thickness.

Flap configurations included 25-, 35-, and 45-percent-chord plain flaps. The flaps extended from the fuselage intersection at $0.20\frac{b}{2}$ to $0.95\frac{b}{2}$ and were divided into three equal $0.25\frac{b}{2}$ segments. These segments were deflected separately and in combinations which gave flap spans equal to 25, 50, and 75 percent of the wing semispan. For the two larger-span flaps, the gaps between increments were sealed and faired to provide continuous spans. Small grooves were machined in the wing at the flap hinge lines, thereby permitting deflection of the flaps about an axis which lay near the lower surface of the wing. (See fig. 2.) Deflections were made from 0° to 15° and were measured normal to the hinge line.

The reference axis of the wing used in the investigation was displaced from the reference axis of the fuselage to provide an exposed wing span that would conform with that of a configuration being investigated at low speeds.

Tests

The present tests were conducted in the Langley 9- by 12-inch supersonic blowdown tunnel, which is of the nonreturn type utilizing the exhaust air of the Langley 19-foot pressure tunnel. The absolute pressure of the inlet air is approximately $2\frac{1}{3}$ atmospheres and contains about 0.3 percent of water by weight. The free-stream Mach number is 1.90. Possible factors in the air-flow characteristics which might affect the aerodynamic results are discussed in reference 2.

The dynamic pressure and the test Reynolds number decreased about 3.5 percent during the course of each run because of the decreasing pressure of the inlet air. The average dynamic pressure for these tests was 11.5 pounds per square inch, and the average Reynolds number was 2.3×10^6.

The aerodynamic characteristics of the wing were determined through a range of flap deflections from 0° to 15° for the various flap configurations. The angle-of-attack range investigated varied from -2° to 4°. Five-component force measurements were obtained on the wing tested in the presence of, but not attached to, a half-fuselage. Because of balance deflections under load, a small gap of approximately 0.015 inch was maintained between model and fuselage under the no-load condition.

TEST TECHNIQUE

In the test arrangement used, the semispan wing model is cantilevered from a strain-gage balance which mounts flush with the tunnel wall and rotates with the model through the angle-of-attack range. The half-fuselage is attached to the housing of the balance system, thus permitting the wing to be tested in the presence of, but not attached to, the fuselage.

The initial program in developing an acceptable technique for testing semispan models in this tunnel was reported in reference 2. It was found that shimming a half-fuselage away from the tunnel wall not only minimized wall-boundary-layer effects over the fuselage but also brought the pressure distribution over the fuselage in better agreement with that measured over a complete fuselage mounted in the center of the tunnel.

It was believed that a more exact means of evaluating the wall-mounting technique would be to investigate the loading carried on a lifting surface in the vicinity of the wing-fuselage juncture. Accordingly, additional development work has been carried out whereby the pressure distribution has been measured on a two-dimensional airfoil extending through a fuselage. To obtain a basis for comparison, data were first obtained with the fuselage mounted in the center of the tunnel (fig. 3). For this arrangement there was no gap (close sliding fit) between the airfoil and fuselage. The fuselage was then split and mounted as a half-fuselage on the tunnel wall in approximately the same arrangement as used in the force tests (shimmed out 0.25 inch with a 0.020-inch clearance gap around the airfoil). The survey airfoil had double-wedge sections and five pressure orifices on both the upper and lower surfaces. It was so arranged as to allow spanwise movement through the fuselage.

The results of these survey tests are presented in figures 4(a) and 4(b) for angles of attack of 0° and 4°, respectively. Pressure measurements presented are for the regions which were not influenced by the Mach cone emanating from the airfoil tip or by the wall-reflected Mach cone from the fuselage nose. (Pressure measurements on the airfoil made on both sides of the fuselage mounted in the center of the tunnel indicated no appreciable effects of the fuselage support strut.)

Qualitative examination of the data of figures 4(a) and 4(b) shows that the airfoil pressures measured for the two fuselage arrangements were in good agreement. However, the use of the shimmed wall-mounted fuselage with a gap around the airfoil caused small deviations to occur in the pressures for a distance of about 1 inch immediately outside the fuselage and near the airfoil trailing edge. This was probably a result of gap effects on the boundary layer near the wing-fuselage juncture. Because of these flow disturbances near the surface of the fuselage, it would be expected that the results of tests with inboard controls would not be so reliable as the results of tests with controls located farther outboard.

It was also evident that the fuselage gap allowed some air loading to be carried over the unexposed portion of the airfoil. Although this gap effect was not considered significant for the range of angles of attack of the present tests, the data indicate that such loads could produce significant effects on the data obtained by this technique at greater angles of incidence.

ACCURACY

Free-stream Mach number has been calibrated at 1.90 ± 0.02. This Mach number was used in determining dynamic pressure. Calibration of the tunnel-clear condition indicated that static pressure varied about ± 1.5 percent in the test-section region.

No tare corrections have been applied to any of the data presented. As shown by the out-of-trim conditions of figure 5, some errors existed in the absolute measurement of the data. Smaller errors, however, existed in the measurements of test points relative to each other and

the magnitudes of these errors, which indicate the accuracy of the cross plots, are believed to be of the following order:

Variable	Error
$\Delta p/q$	±0.002
α, degrees	±0.05
δ, degrees	±0.10
C_l	±0.001
C_L	±0.005
C_D	±0.001
C_m	±0.002
C_n	±0.0002

Twist in the survey airfoil due to inaccuracies in fabrication caused a variation in angle of attack that amounted to less than ±0.2°. Considering this variation, the absolute values of $\frac{\Delta p}{q}$ are believed to be accurate to ±0.01.

RESULTS

Complete test data for the wing with 25-percent-chord flaps are presented in figures 5 to 9 where the aerodynamic coefficients are plotted against angle of attack for the various configurations. These plots are representative of the experimental data; therefore, the corresponding plots for the 35- and 45-percent-chord flaps are omitted. Displacement of the curves for the basic wing (flaps neutral) presented in figures 5(a) and 5(c) is believed to have been caused by model misalinement and slight changes in the wing-fuselage incidence resulting from variations in the test setups. Therefore, when changes in the setups were necessary, additional basic wing tests were made and used for the subsequent series of tests.

Cross plots of the basic data are presented in figures 10 to 13 in which the coefficients are plotted against flap deflection at zero angle of attack. Symbols were used in these plots to show clearly the trends of the aerodynamic coefficients and the points taken from the unpresented data. Additional cross plots of C_{l_δ} against $\frac{b_f}{b/2}$, $\frac{y_f}{b/2}$, and $\frac{c_f}{c}$ and of C_{L_δ} against $\frac{b_f}{b/2}$ and $\frac{c_f}{c}$ are presented in figures 14 to 16.

The experimental and calculated theoretical results are summarized in table I. The theoretical results were calculated by the method described in references 3 and 4.

DISCUSSION

Wing Characteristics

The experimental value of C_{L_α} for the wing was about 0.0425 (fig. 6(a)) as compared with the theoretical value of 0.0445 calculated by the method described in reference 3 with a correction for fuselage upwash applied using the method described in reference 5. From figure 5(a), the rate of change of $C_{l_{gross}}$ with angle of attack was equal to about 0.0056. The theoretical value, obtained by using references 3 and 5 was 0.0057. The minimum drag coefficient for the wing in the presence of the fuselage was about 0.019 (fig. 7(a)). Based on the experimental lift and pitching-moment data, the chordwise location of the center of pressure was calculated to be about 8 percent of the wing mean aerodynamic chord ahead of the center of area.

Flap Characteristics

Rolling moment.- Figure 5 shows that, for the small angle-of-attack range covered, the rolling effectiveness of the flaps was independent of angle of attack. The values of the rolling-moment coefficient obtained from figure 10 varied linearly for each flap throughout the deflection range and were approximately additive for the individual flap spans. The data of figure 14 show a decrease in the value of the rolling-effectiveness parameter C_{l_δ} with inboard movement of a constant-span flap. There was also a decrease in the rate of change of C_{l_δ} with span as the span decreased for a given value of the spanwise-location parameter $\frac{y_f}{b/2}$. This decrease follows the same trends evidenced in the change in flap area moments (about the rolling-moment reference axis) with flap span. The data of figure 15 indicate a slight increase in the rate of change of C_{l_δ} with flap chord as the chord increased. A study of table I shows that, for this wing-flap arrangement at a Mach number of 1.9, the theoretical effectiveness values are not appreciably affected by flow conditions at the flap ends, since for each flap chord the summation of the theoretical values of C_{l_δ} for various combinations of the flap-span segments agree within 1 percent with the value calculated for flaps deflected as a unit. Summation of experimental values, however, did not agree as well and deviated as much as 10 percent. This lack of agreement indicates that single spanwise effectiveness curves for a given flap chord would not be completely accurate. (See fig. 14(b).) The trends predicted by theory (figs. 14(a), 14(b), and 15) agreed qualitatively with

those noted experimentally; however, for most arrangements the theoretical values of C_{l_δ} (table I(a)) were from 10 to 30 percent higher than experiment. These theoretical values possibly are higher as a result of the theoretical assumptions of unseparated flow on the model and no gap leakage at the ends of the deflected flaps. The results for the 25-percent-span flaps located adjacent to the fuselage were an exception in that the theoretical effectiveness sometimes fell below the measured effectiveness, and this difference increased as the chord increased. This result was attributed to limitations of theory which did not consider the increased rate of flow near the fuselage (illustrated in the pressure-distribution data of fig. 4).

Lift and pitching moment.- Lift effectiveness was constant through the angle-of-attack range (fig. 6). In view of the estimated accuracy of the data in figure 11, only one curve was faired through the points obtained for a given span flap located at various spanwise positions. Figure 11 shows that the increments in lift coefficient caused by flap deflection varied linearly with flap deflection throughout the deflection range and were about additive for combinations of the flap-span segments. The data of figure 16 indicate that the lift-effectiveness parameter C_{L_δ} was approximately a linear function of flap span and that an increase generally occurred in the rate of change of C_{L_δ} with flap chord as the chord increased. The results show that, for a given increase in flap area, increasing the flap chord rather than the span would provide a slightly greater value of C_{L_δ}. Theory predicted about the same trends as indicated by the experimental results, although the theoretical values of C_{L_δ} (table I(b)) ranged from 0 to 30 percent higher than experiment.

Deflecting the flaps shifted the position of the pitching-moment curves in a negative direction (fig. 8) but did not alter the slope. The data of figure 12(b) indicated a linear variation of pitching moment with flap deflection. The theoretical values of the pitching-moment parameter C_{m_δ} (table I(c)) were from 0 to 30 percent higher than experimental results, except for some inboard-flap configurations where theoretical effectiveness was shown to be too low. These differences were probably due to the flow-field characteristics near the fuselage as discussed in the section on rolling moment.

CONCLUSIONS

From tests in the Langley 9- by 12-inch supersonic blowdown tunnel at a Mach number of 1.9 to determine the effects of size and location

of plain flaps on an unswept low-aspect-ratio wing, the following conclusions may be drawn:

1. The values of the rolling-moment coefficient varied linearly with flap deflection and were about additive for the various flap configurations. The rate of change in the rolling-effectiveness parameter C_{l_δ} with flap span, brought about by progressive removal of the outboard end of the flap, decreased slightly as the span decreased. A slight increase was noted in the rate of change of C_{l_δ} with flap chord as the chord increased.

2. The increments in lift coefficient caused by flap deflection varied linearly with flap deflection throughout the deflection range and were approximately additive for adjacent flap-span segments. Lift effectiveness varied linearly with flap span; however, an increase in the rate of change of effectiveness with flap chord was noted as the chord increased.

3. Theory predicted qualitatively the trends in control effectiveness characteristics as influenced by flap deflection, size, and location. Calculated effectiveness values were higher than the experimental results by 10 to 30 percent for rolling moment and 0 to 30 percent for lift and pitching moment, except for flaps having areas located adjacent to the fuselage. For such configurations, the calculated effectiveness sometimes fell below experiment, probably because theory did not consider the increased rate of flow near the fuselage.

Langley Aeronautical Laboratory
National Advisory Committee for Aeronautics
Langley Air Force Base, Va.

REFERENCES

1. Strass, H. Kurt: The Effect of Spanwise Aileron Location on the Rolling Effectiveness of Wings with 0° and 45° Sweep at Subsonic, Transonic, and Supersonic Speeds. NACA RM L50A27, 1950.

2. Conner, D. William: Aerodynamic Characteristics of Two All-Movable Wings Tested in the Presence of a Fuselage at a Mach Number of 1.9. NACA RM L8H04, 1948.

3. Lagerstrom, P. A., Wall, D., and Graham, M. E.: Formulas in Three-Dimensional Wing Theory. Rept. No. SM-11901, Douglas Aircraft Co., Inc., July 8, 1946.

4. Lagerstrom, P. A., and Graham, Martha E.: Linearized Theory of Supersonic Control Surfaces. Jour. Aero. Sci., vol. 16, no. 1, Jan. 1949, pp. 31-34.

5. Beskin, L.: Determination of Upwash around a Body of Revolution at Supersonic Velocities. Rep. No. APL/JHU-CM-251, The John Hopkins Univ., Appl. Phys. Lab., May 27, 1946.

TABLE I

EXPERIMENTAL AND CALCULATED FLAP CHARACTERISTICS OF A

WING MODEL AT A MACH NUMBER OF 1.9

(a) Rolling-effectiveness parameter, C_{l_δ}

Flap span (percent b/2)	Location of inboard end of flap (percent b/2)	C_{l_δ}					
		$\frac{c_f}{c} = 0.25$		$\frac{c_f}{c} = 0.35$		$\frac{c_f}{c} = 0.45$	
		Exp.	Calc.	Exp.	Calc.	Exp.	Calc.
75	20	0.00087	0.00104	0.00124	0.00153	0.00180	0.00207
50	45	.00066	.00083	.00104	.00123	.00141	.00168
	20	.00048	.00058	.00070	.00085	.00099	.00114
25	70	.00042	.00046	.00056	.00069	.00079	.00094
	45	.00029	.00037	.00044	.00054	.00062	.00074
	20	.00018	.00021	.00032	.00031	.00044	.00040

NACA

TABLE I

EXPERIMENTAL AND CALCULATED FLAP CHARACTERISTICS OF A

WING MODEL AT A MACH NUMBER OF 1.9 - Continued

(b) Lift-effectiveness parameter, C_{L_δ}

Flap span (percent b/2)	Location of inboard end of flap (percent b/2)	C_{L_δ}					
		$\frac{c_f}{c} = 0.25$		$\frac{c_f}{c} = 0.35$		$\frac{c_f}{c} = 0.45$	
		Exp.	Calc.	Exp.	Calc.	Exp.	Calc.
75	20	0.0063	0.0074	0.0104	0.0109	0.0136	0.0145
50	45	.0040	.0048	.0064	.0072	.0088	.0098
	20	.0040	.0051	.0064	.0075	.0088	.0100
25	70	.0021	.0023	.0032	.0034	.0046	.0046
	45	.0021	.0026	.0032	.0038	.0046	.0052
	20	.0021	.0026	.0032	.0037	.0046	.0047

NACA

TABLE I

EXPERIMENTAL AND CALCULATED FLAP CHARACTERISTICS OF A

WING MODEL AT A MACH NUMBER OF 1.9 - Concluded

(c) Pitching-moment parameter, C_{m_δ}

Flap span (percent b/2)	Location of inboard end of flap (percent b/2)	C_{m_δ}					
		$\frac{c_f}{c} = 0.25$		$\frac{c_f}{c} = 0.35$		$\frac{c_f}{c} = 0.45$	
		Exp.	Calc.	Exp.	Calc.	Exp.	Calc.
75	20	-0.0025	-0.0028	-0.0031	-0.0034	-0.0035	-0.0037
50	45	-.0015	-.0017	-.0019	-.0022	-.0021	-.0024
	20	-.0018	-.0020	-.0025	-.0025	-.0028	-.0027
25	70	-.0007	-.0008	-.0008	-.0010	-.0008	-.0011
	45	-.0009	-.0010	-.0011	-.0012	-.0012	-.0014
	20	-.0012	-.0011	-.0014	-.0013	-.0012	-.0013

NACA

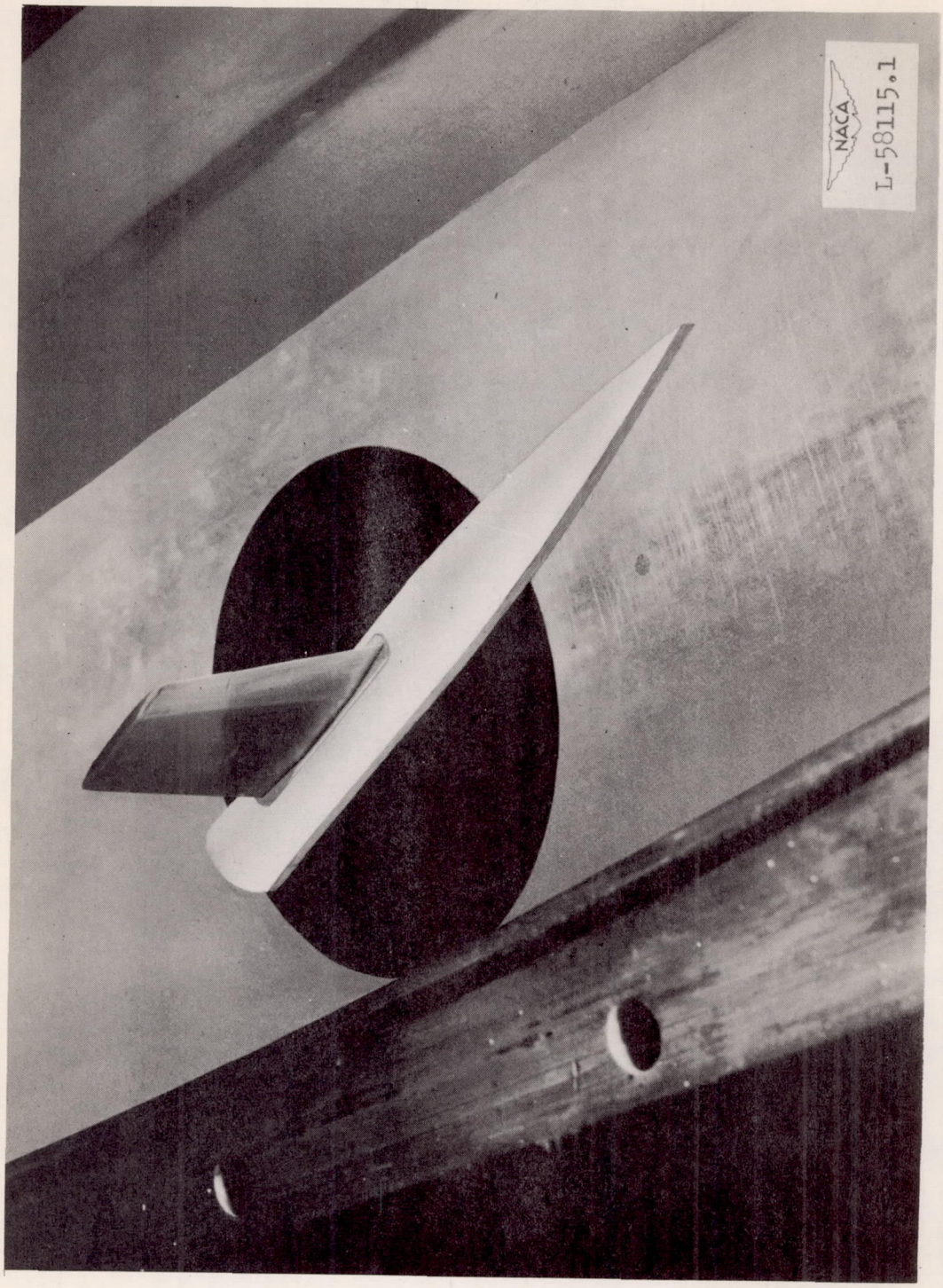

Figure 1.- Photograph of semispan wing model.

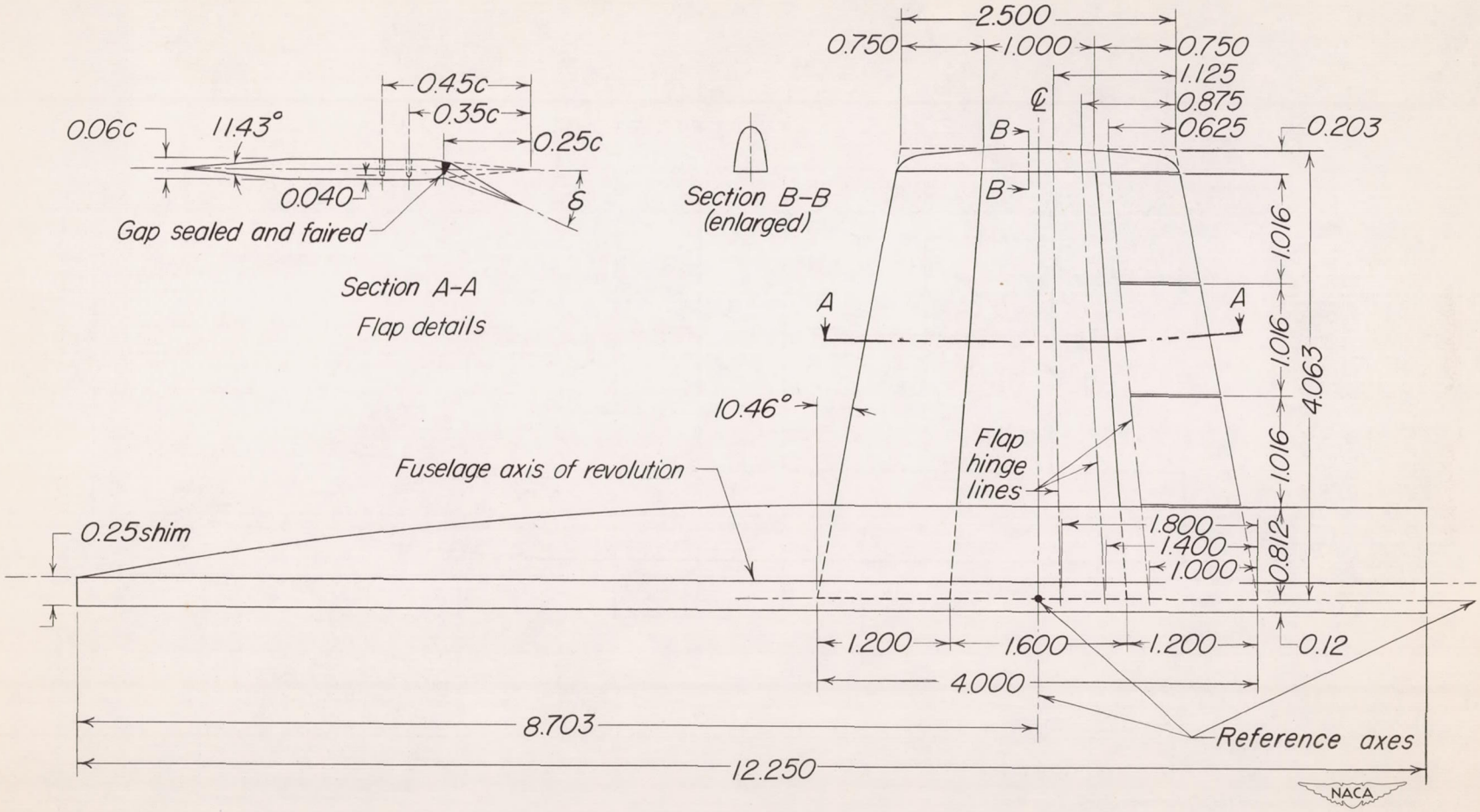

Figure 2.- Details of semispan wing model. All dimensions in inches.

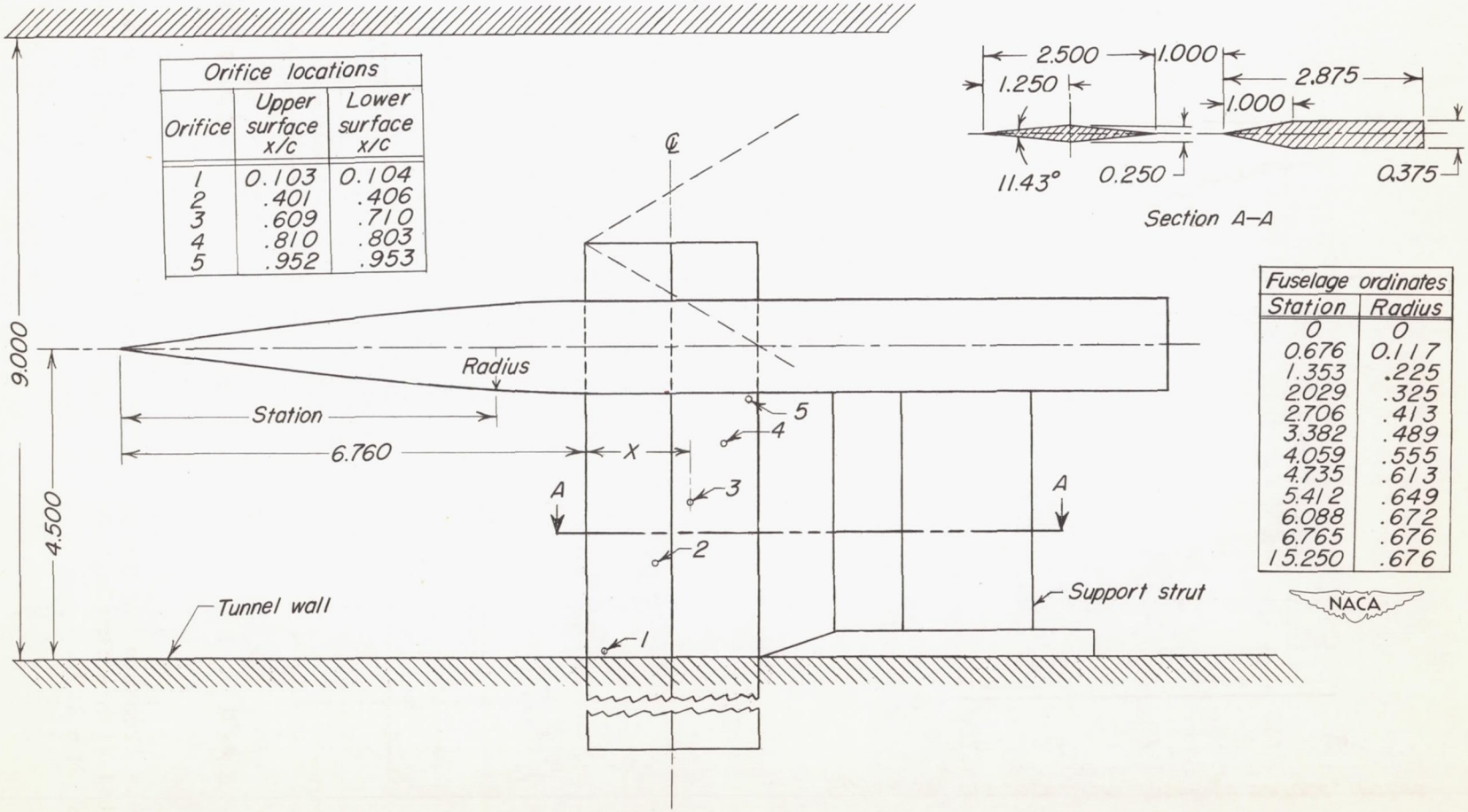

Figure 3.- Details of survey airfoil and fuselage. All dimensions in inches.

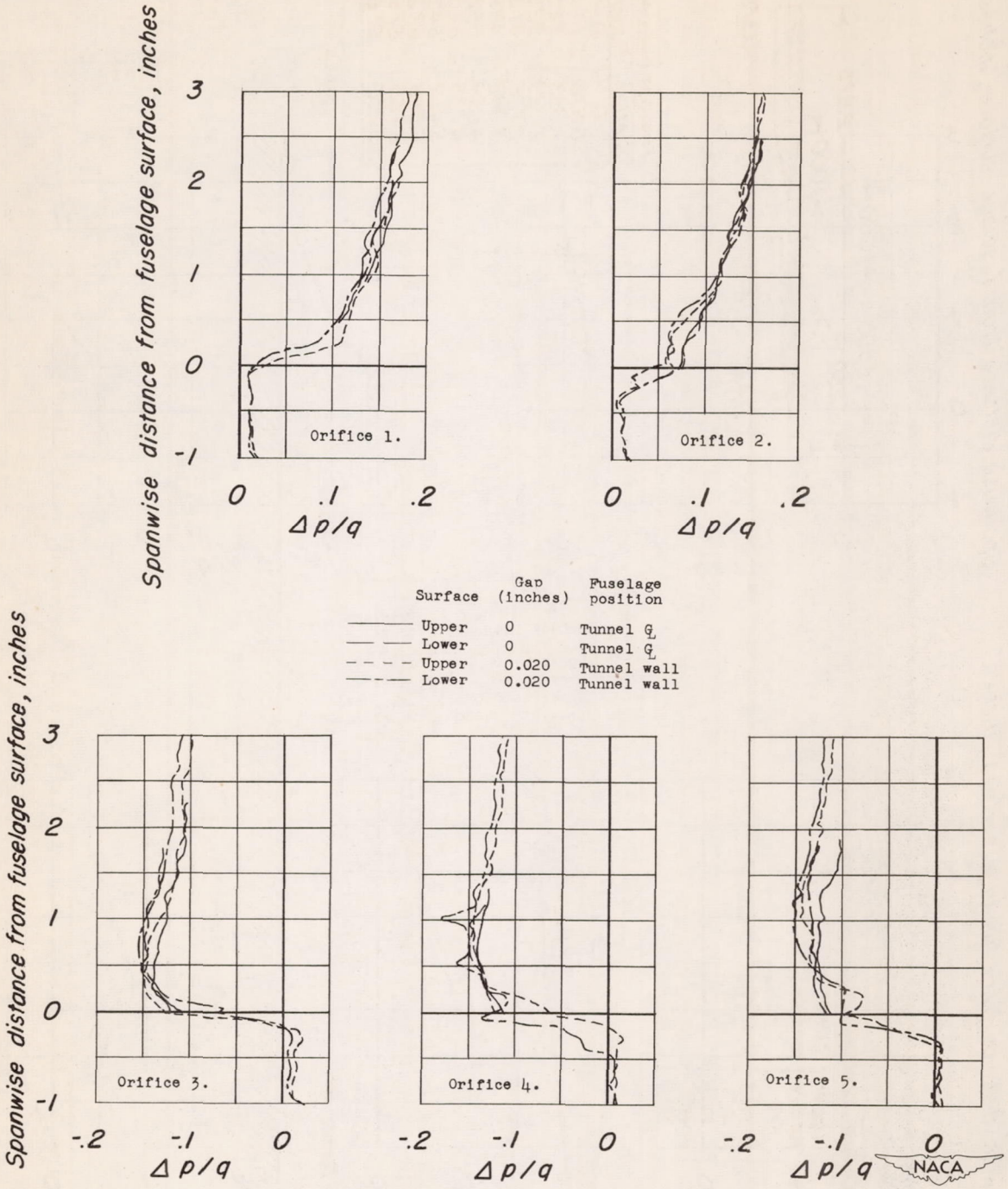

(a) Airfoil at $\alpha = 0^{\circ}$.

Figure 4.- Pressure-coefficient characteristics of a double-wedge airfoil mounted with a fuselage in the center of the tunnel and on the tunnel wall. M = 1.90.

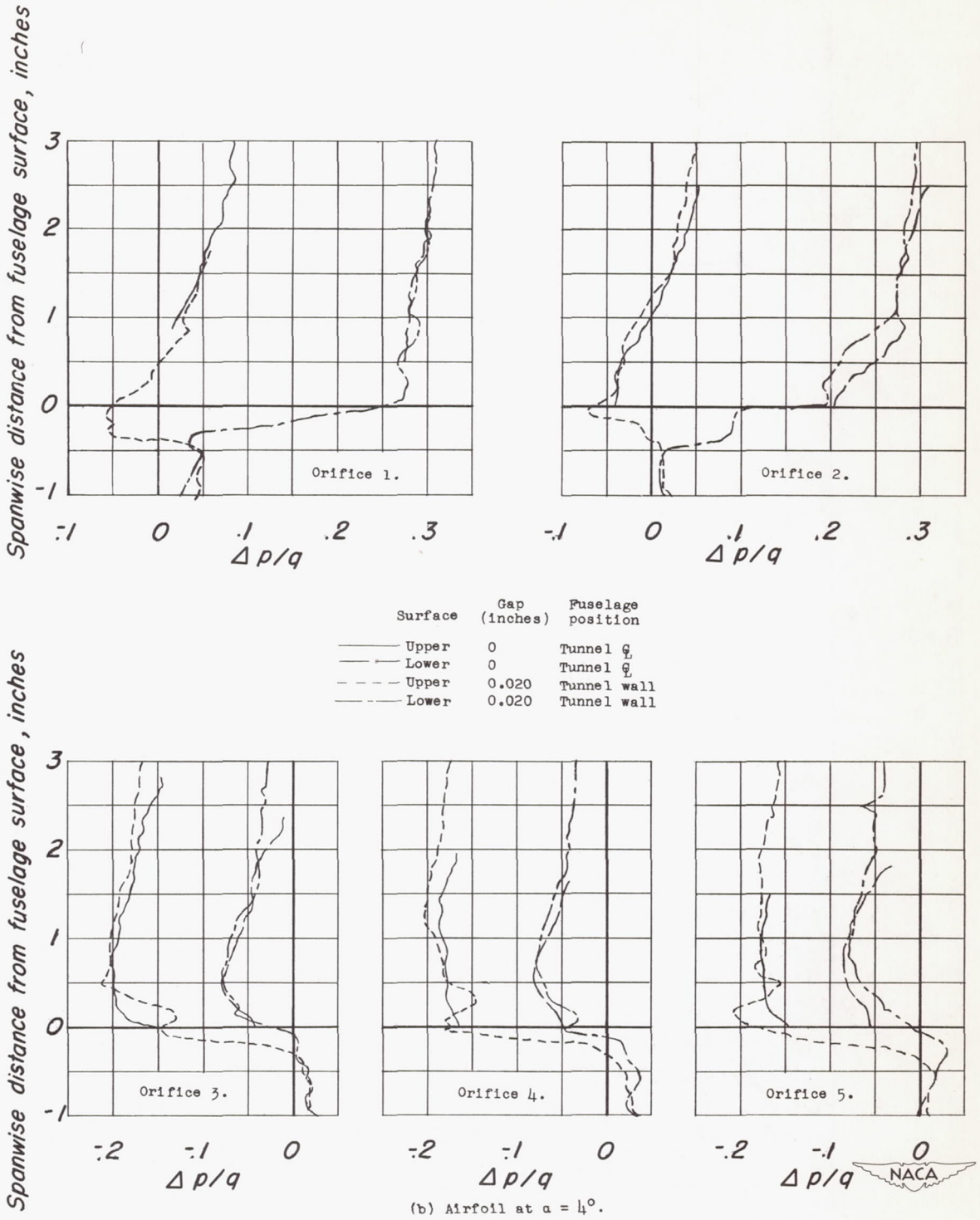

(b) Airfoil at $\alpha = 4^{\circ}$.

Figure 4.- Concluded.

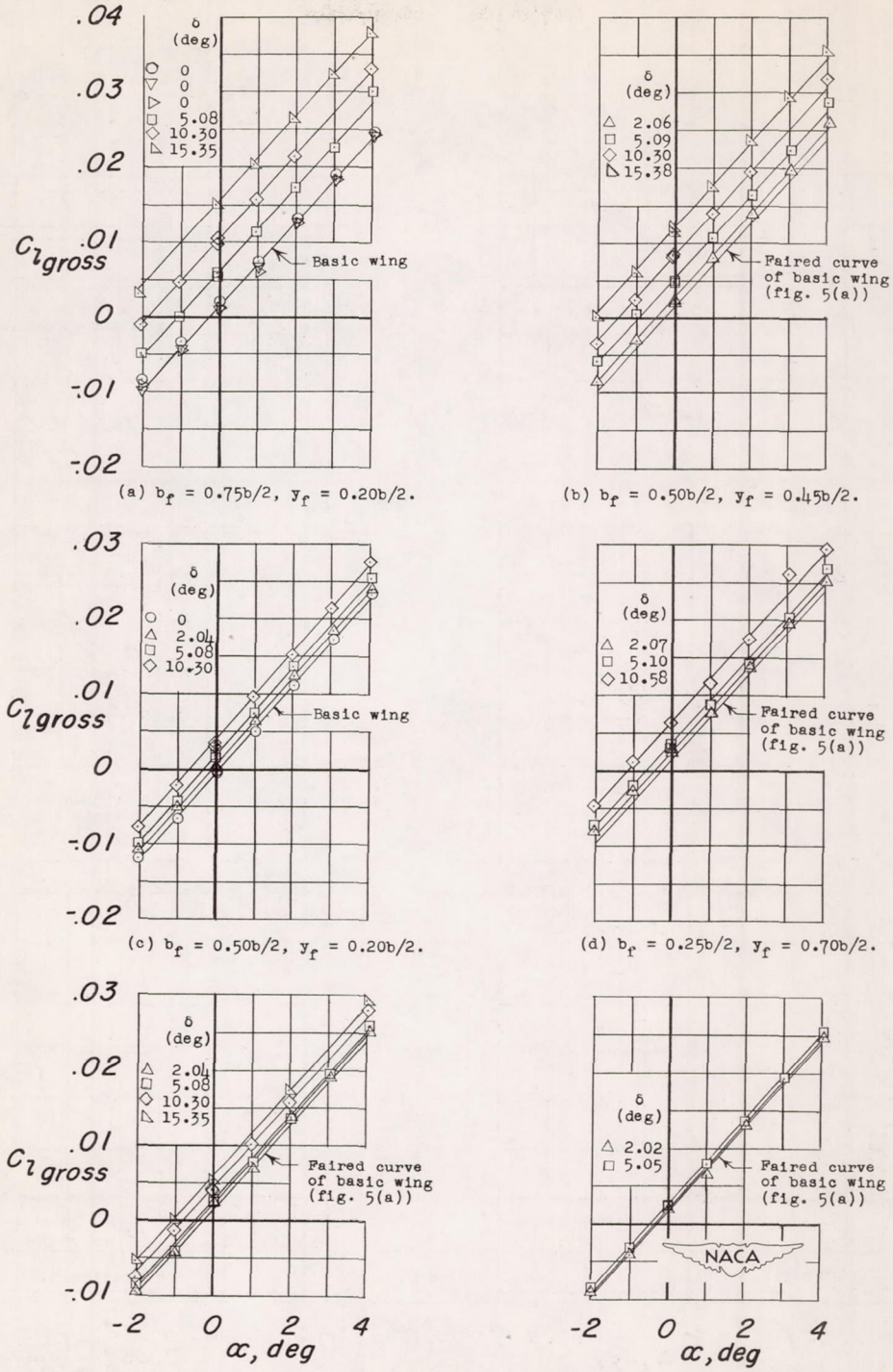

Figure 5.- Rolling-moment characteristics of a semispan wing with 25-percent-chord flaps. $R = 2.3 \times 10^6$; $M = 1.9$.

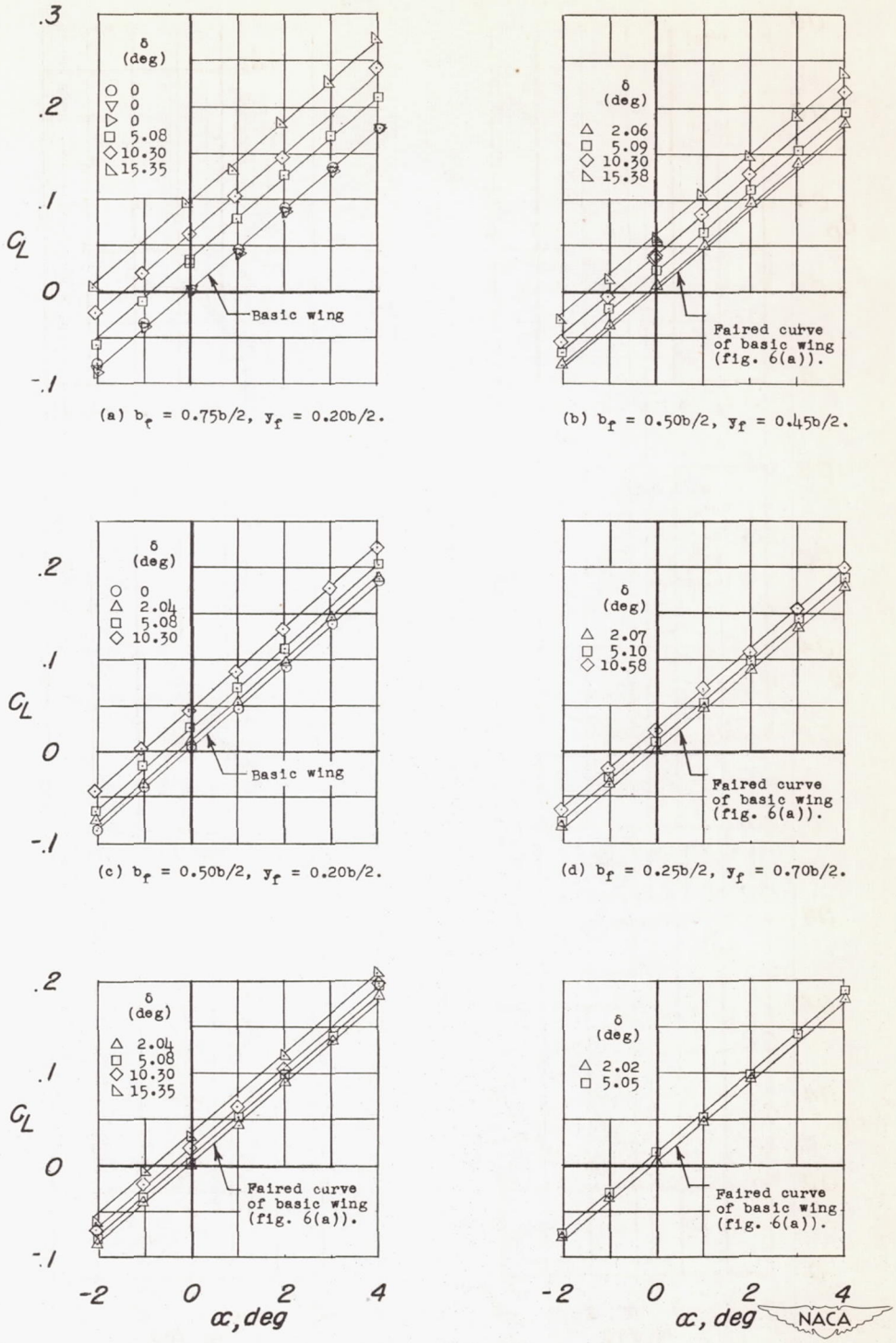

(a) $b_f = 0.75b/2$, $y_f = 0.20b/2$.

(b) $b_f = 0.50b/2$, $y_f = 0.45b/2$.

(c) $b_f = 0.50b/2$, $y_f = 0.20b/2$.

(d) $b_f = 0.25b/2$, $y_f = 0.70b/2$.

(e) $b_f = 0.25b/2$, $y_f = 0.45b/2$.

(f) $b_f = 0.25b/2$, $y_f = 0.20b/2$.

Figure 6.- Lift characteristics of a semispan wing with 25-percent-chord flaps. $R = 2.3 \times 10^6$; $M = 1.9$.

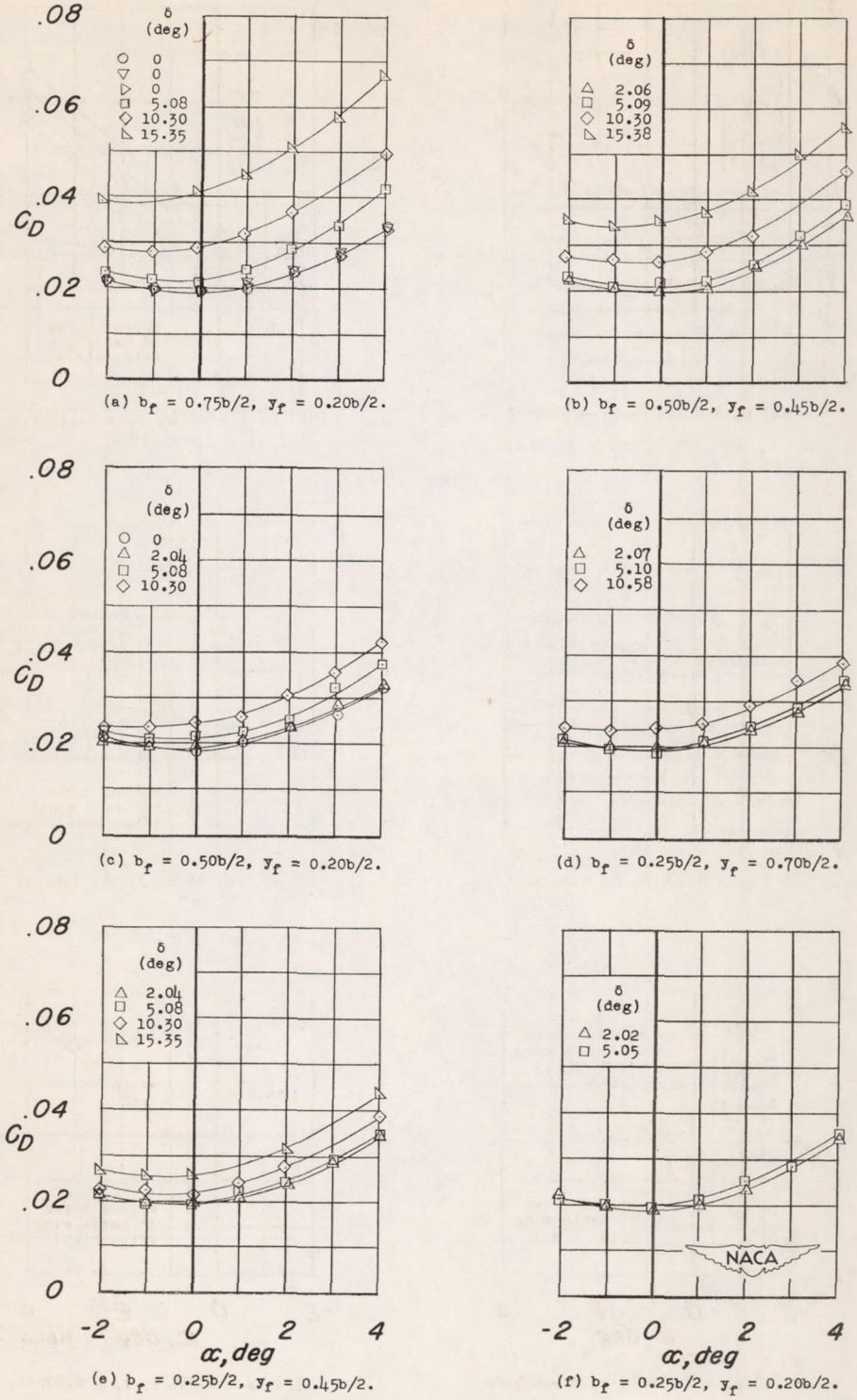

Figure 7.- Drag characteristics of a semispan wing with 25-percent-chord flaps. $R = 2.3 \times 10^6$; $M = 1.9$.

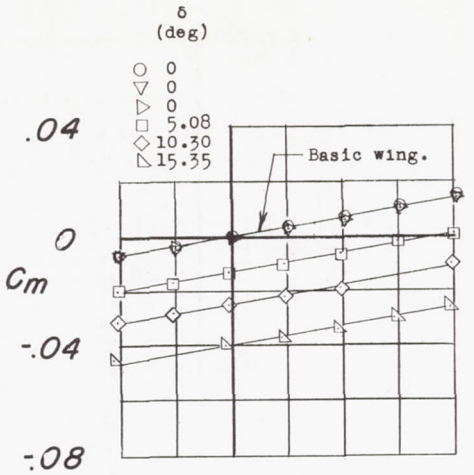

(a) $b_f = 0.75b/2$, $y_f = 0.20b/2$.

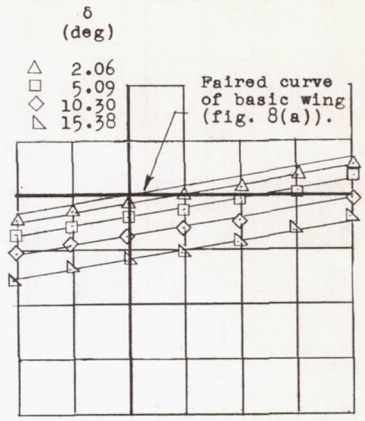

(b) $b_f = 0.50b/2$, $y_f = 0.45b/2$.

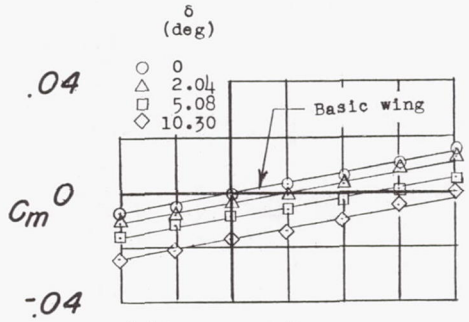

(c) $b_f = 0.50b/2$, $y_f = 0.20b/2$.

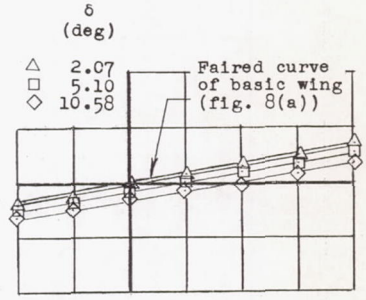

(d) $b_f = 0.25b/2$, $y_f = 0.70b/2$.

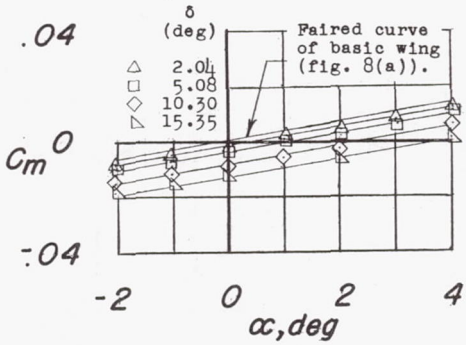

(e) $b_f = 0.25b/2$, $y_f = 0.45b/2$.

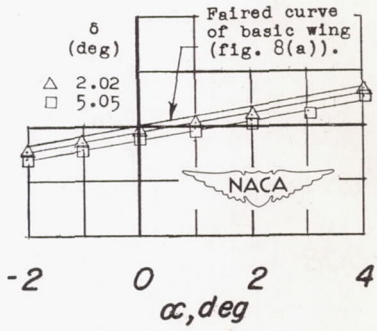

(f) $b_f = 0.25b/2$, $y_f = 0.20b/2$.

Figure 8.- Pitching-moment characteristics of a semispan wing with 25-percent-chord flaps. $R = 2.3 \times 10^6$; $M = 1.9$.

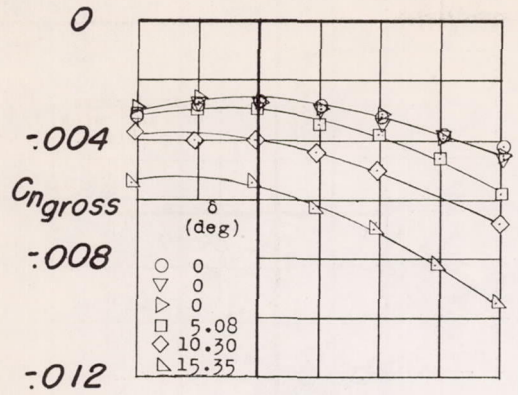

(a) $b_f = 0.75b/2$, $y_f = 0.20b/2$.

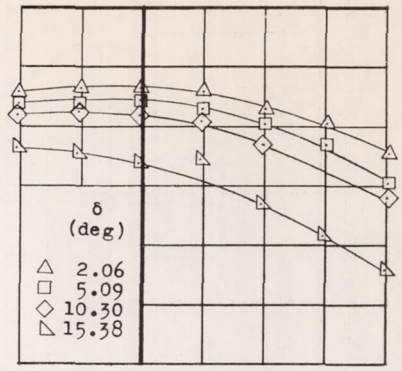

(b) $b_f = 0.50b/2$, $y_f = 0.45b/2$.

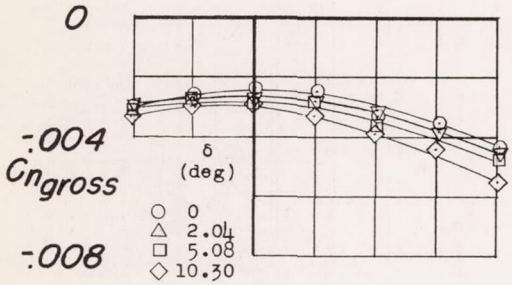

(c) $b_f = 0.50b/2$, $y_f = 0.20b/2$.

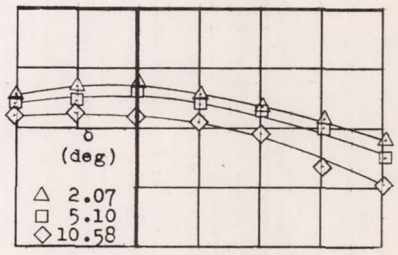

(d) $b_f = 0.25b/2$, $y_f = 0.70b/2$.

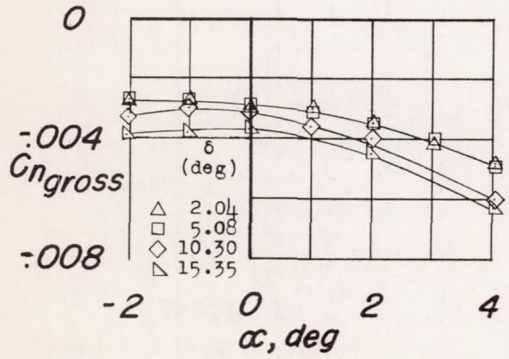

(e) $b_f = 0.25b/2$, $y_f = 0.45b/2$.

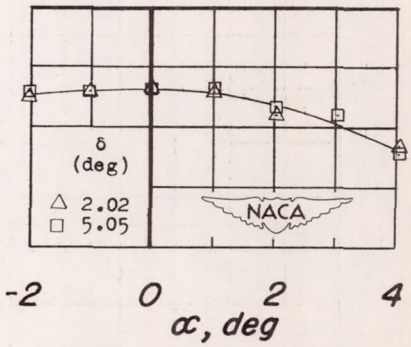

(f) $b_f = 0.25b/2$, $y_f = 0.20b/2$.

Figure 9.- Yawing-moment characteristics of a semispan wing with 25-percent-chord flaps. $R = 2.3 \times 10^6$; $M = 1.9$.

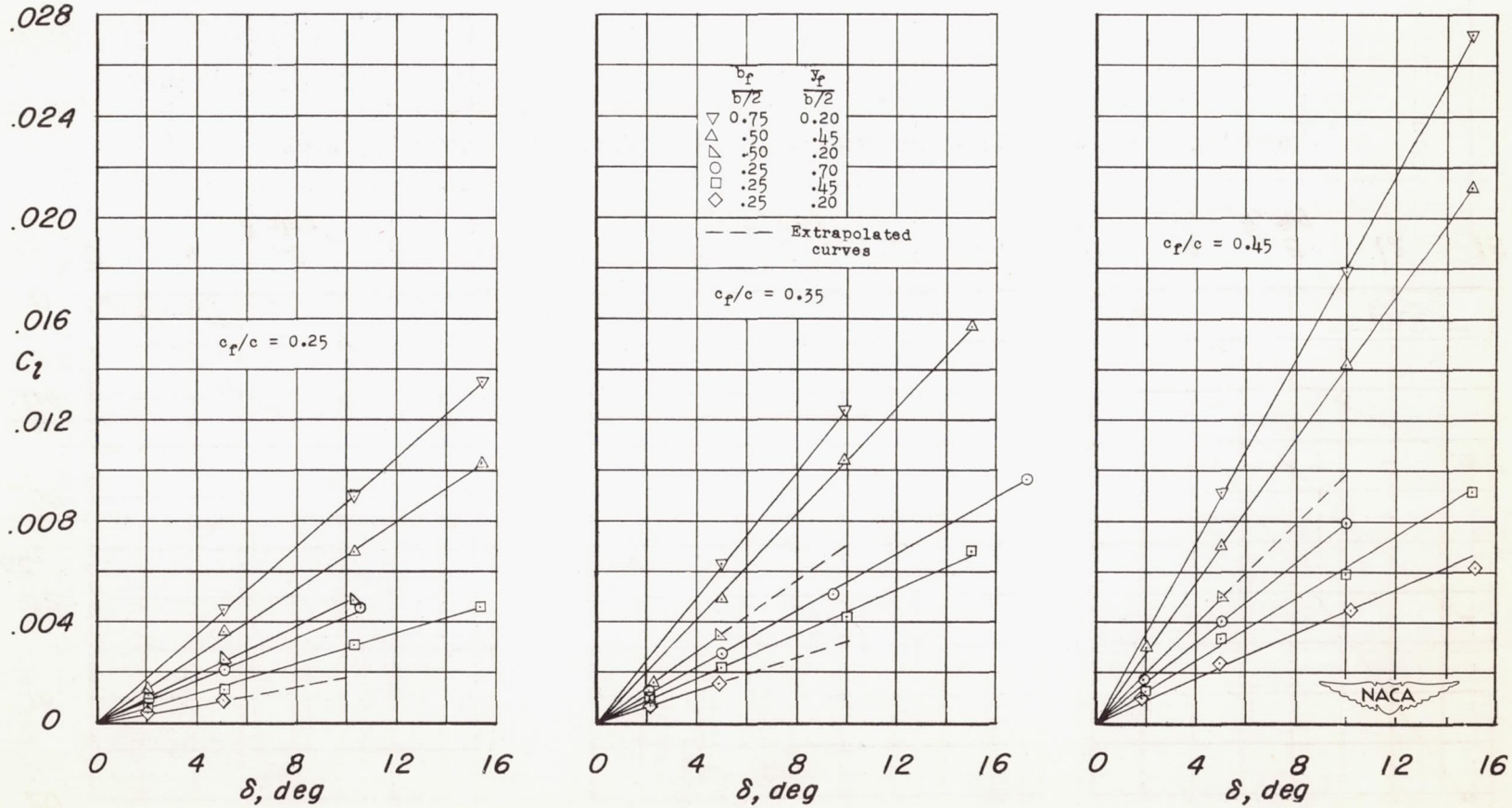

Figure 10.- Rolling-moment characteristics of a semispan wing with 25-, 35-, and 45-percent-chord flaps. $R = 2.3 \times 10^6$; $M = 1.9$; $\alpha = 0^\circ$.

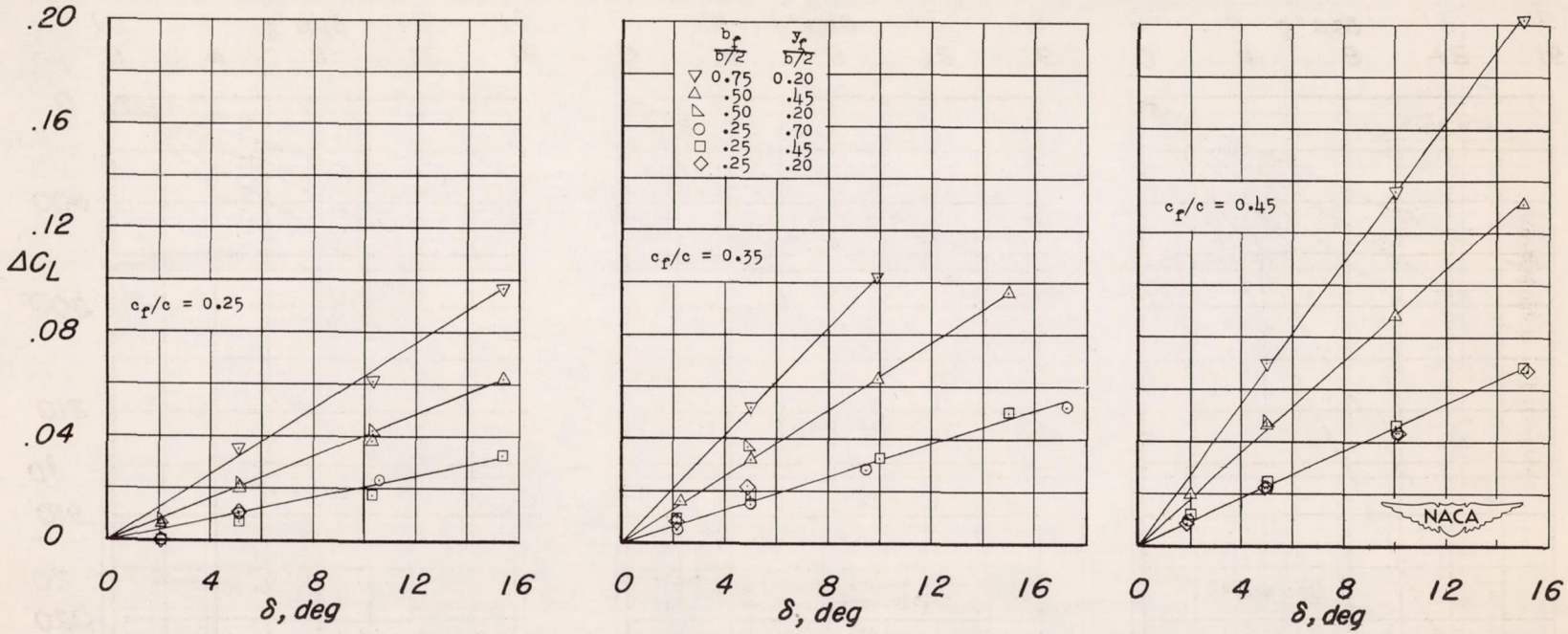

Figure 11.- Lift characteristics of a semispan wing with 25-, 35-, and 45-percent-chord flaps. $R = 2.3 \times 10^6$; $M = 1.9$; $\alpha = 0^\circ$.

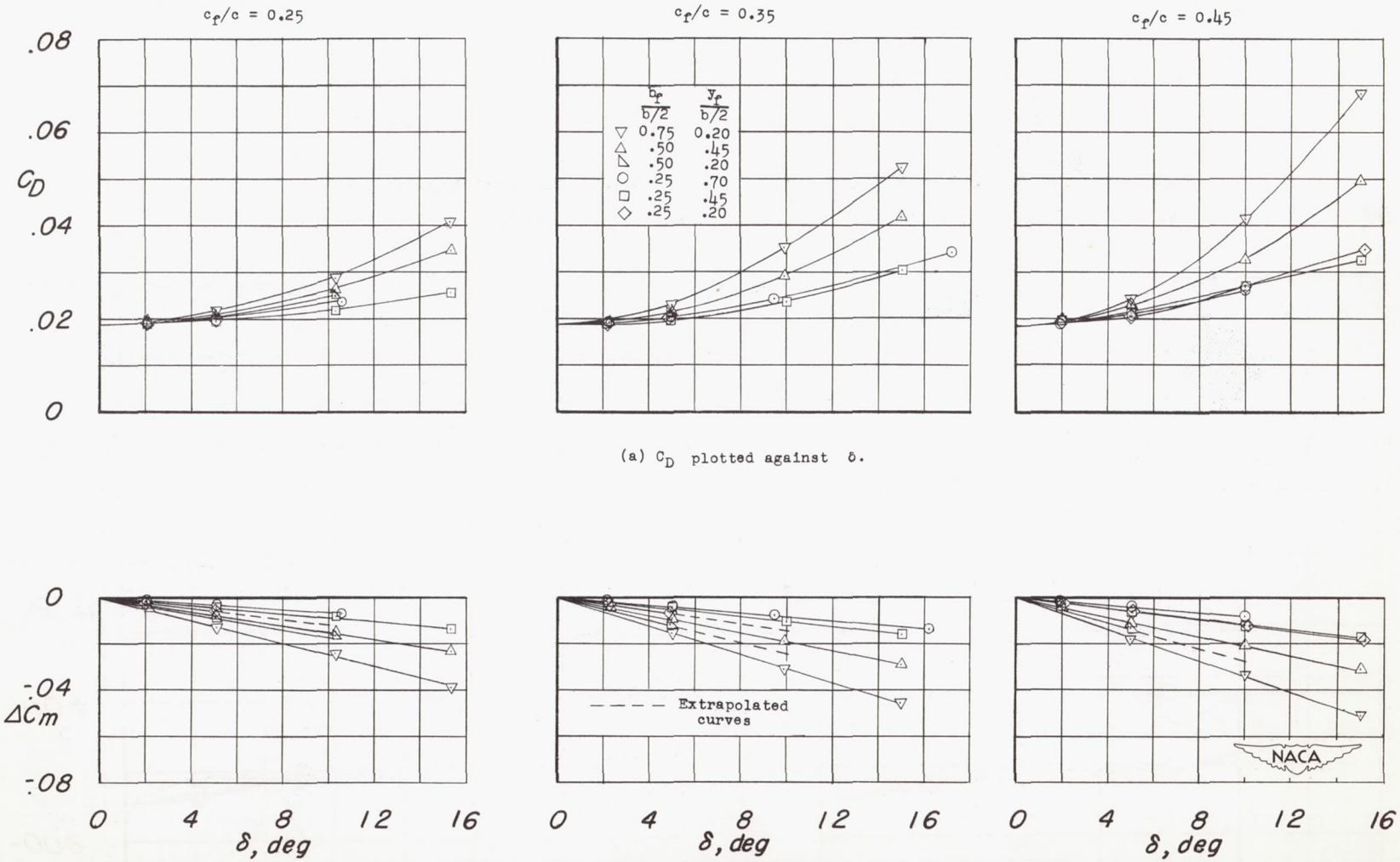

(a) C_D plotted against δ.

(b) ΔC_m plotted against δ.

Figure 12.- Drag and pitching-moment characteristics of a semispan wing with 25-, 35-, and 45-percent-chord flaps. $R = 2.3 \times 10^6$; $M = 1.9$; $\alpha = 0^\circ$.

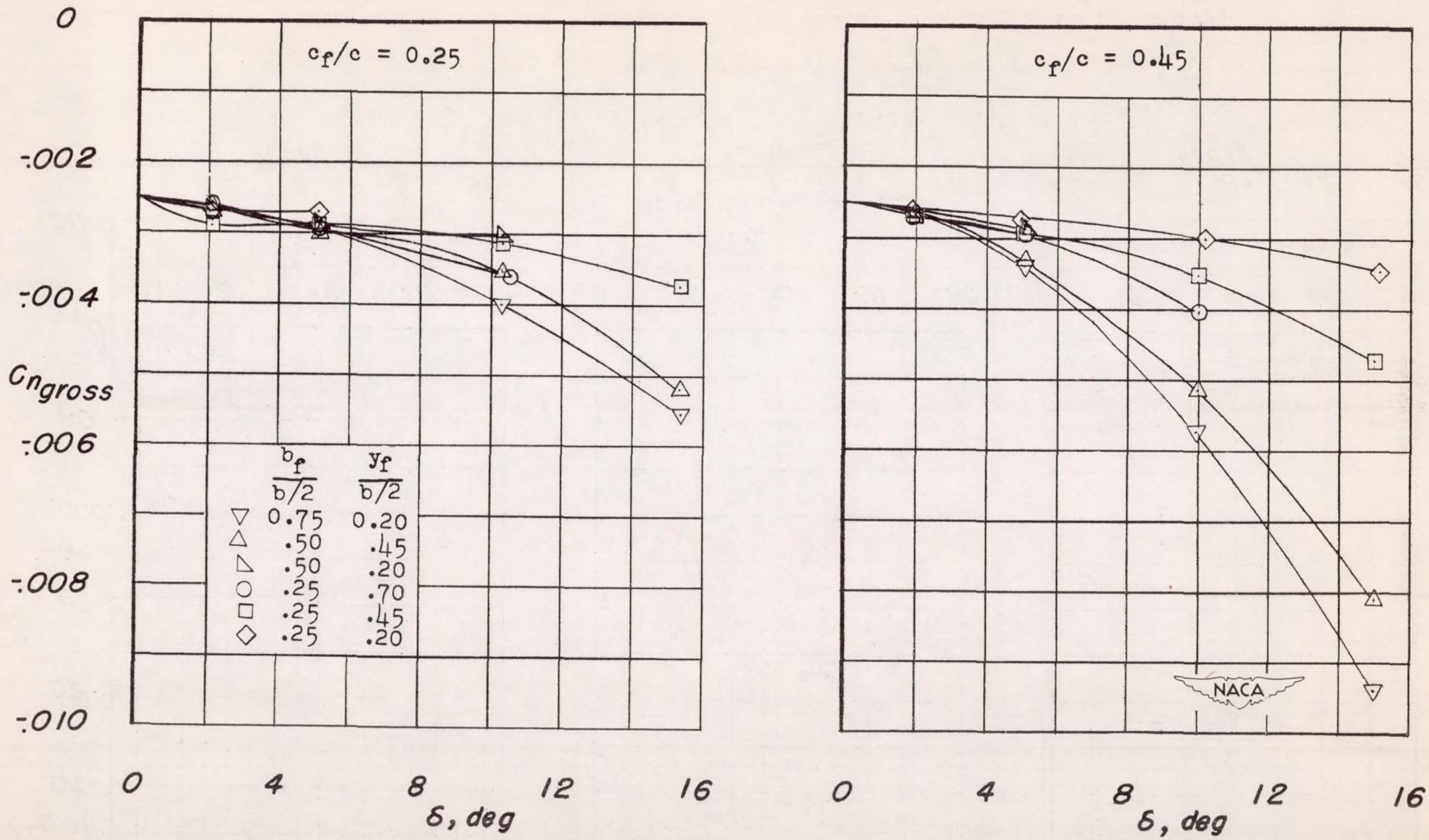

Figure 13.- Yawing-moment characteristics of a semispan wing with 25- and 45-percent-chord flaps. $R = 2.3 \times 10^6$; $M = 1.9$; $\alpha = 0^\circ$.

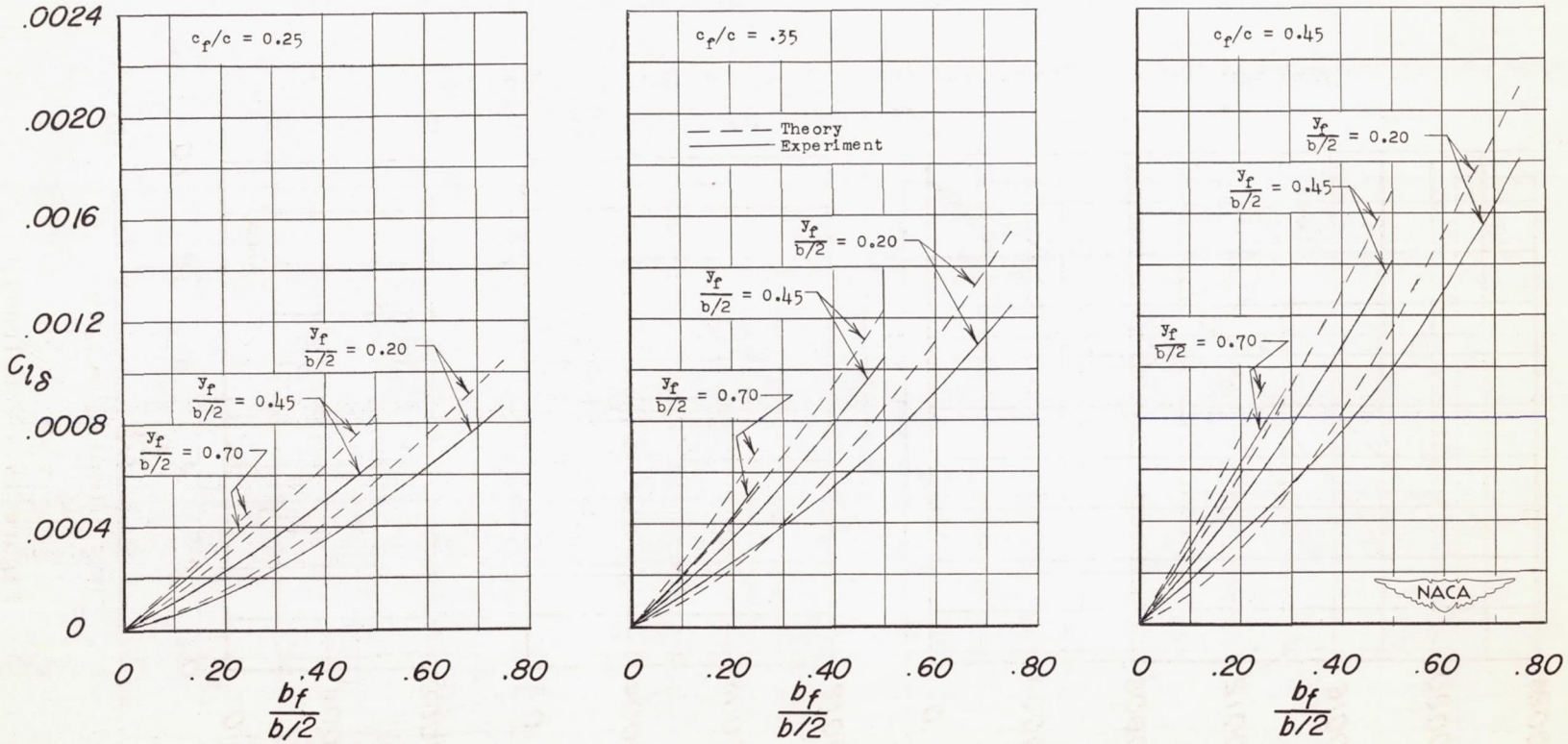

(a) C_{l_δ} plotted against $\frac{b_f}{b/2}$.

Figure 14.- Effects of the span and spanwise location on C_{l_δ}.

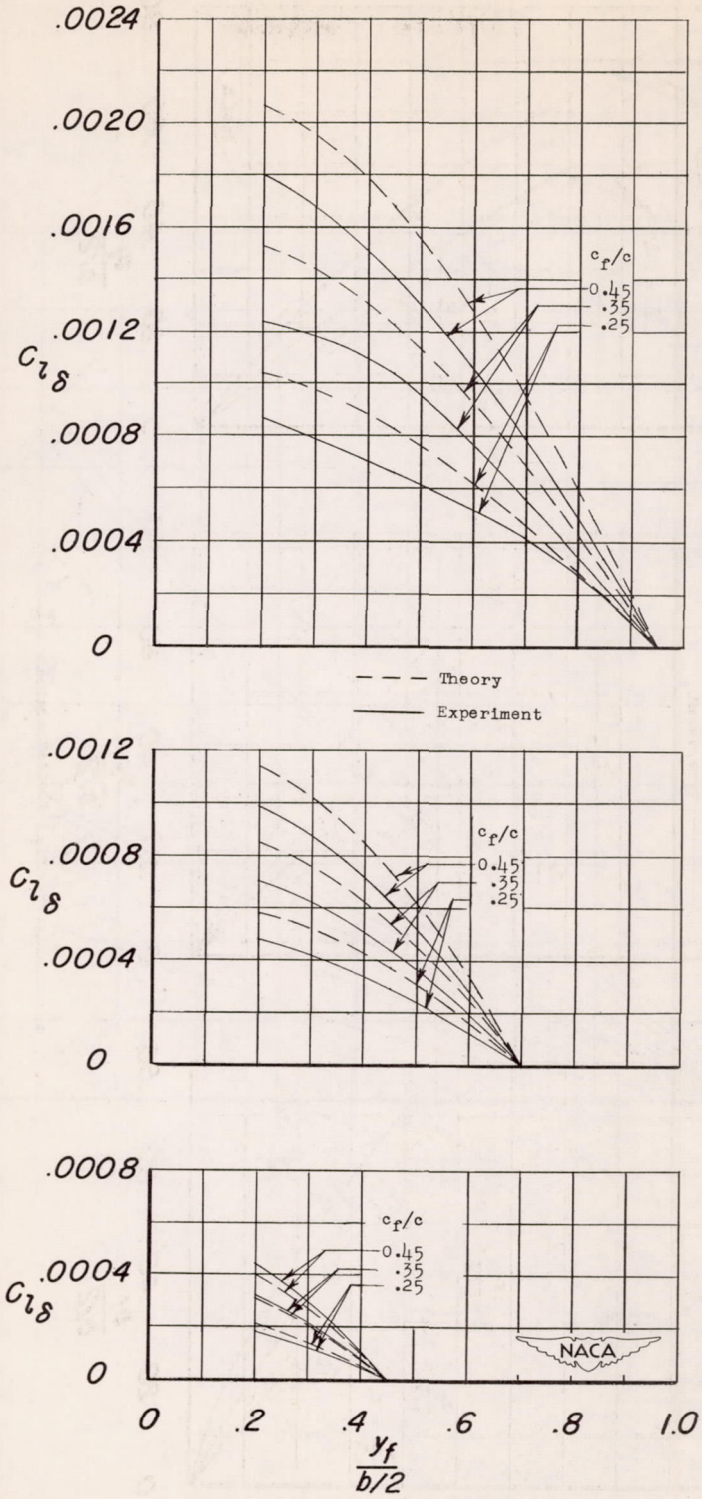

(b) C_{l_δ} plotted against $y_f/b/2$.

Figure 14.- Concluded.

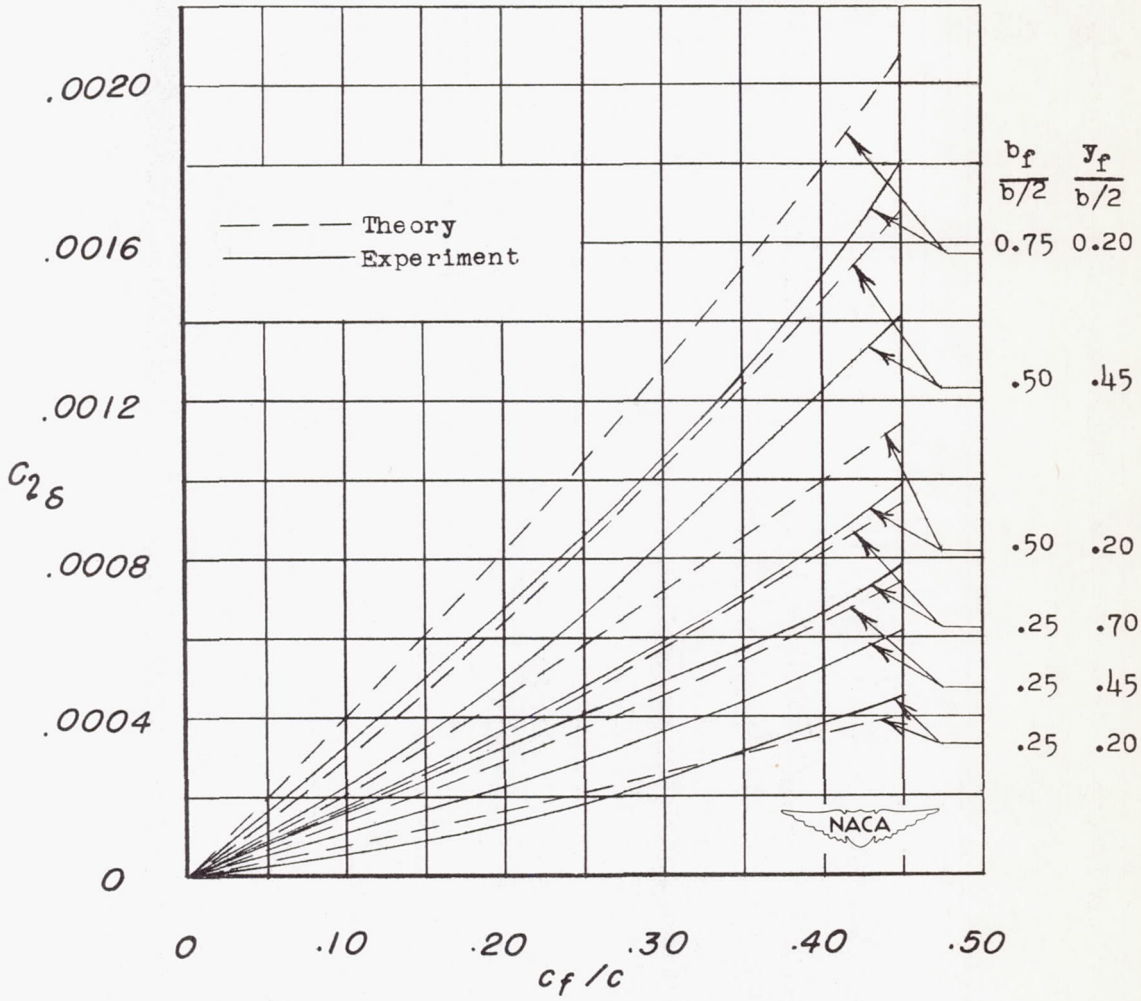

Figure 15.- Effects of flap chord on C_{l_δ}.

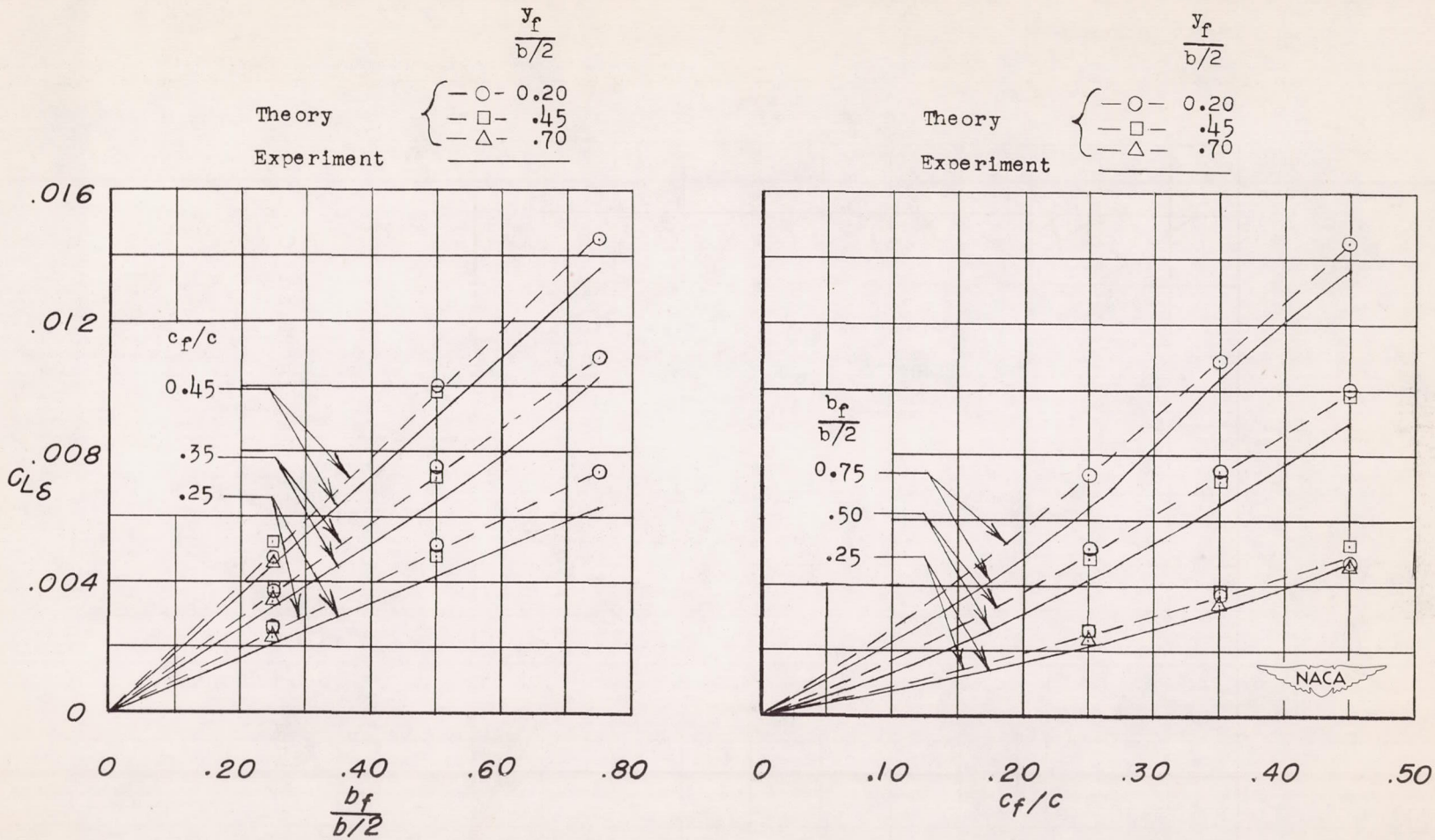

(a) C_{L_δ} plotted against $\frac{b_f}{b/2}$.

(b) C_{L_δ} plotted against c_f/c.

Figure 16.- Effects of flap span, spanwise location, and chord on C_{L_δ}.